EFDA-JET-CP(06)04-09

S.Garavaglia, A.Simonetto, C.Sozzi and JET-EFDA contributors

Mechanical Realization of a Multichanel Martin Puplett Interferometer for Perpendicular and Oblique ECE Measurements on JET

"This document is intended for publication in the open literature. It is made available on the understanding that it may not be further circulated and extracts or references may not be published prior to publication of the original when applicable, or without the consent of the Publications Officer, EFDA, Culham Science Centre, Abingdon, Oxon, OX14 3DB, UK."

"Enquiries about Copyright and reproduction should be addressed to the Publications Officer, EFDA, Culham Science Centre, Abingdon, Oxon, OX14 3DB, UK."

Mechanical Realization of a Multichanel Martin Puplett Interferometer for Perpendicular and Oblique ECE Measurements on JET

S.Garavaglia, A.Simonetto, C.Sozzi and JET-EFDA contributors*

IFP-CNR, Assoc. EURATOM-ENEA-CNR sulla Fusione, v. Cozzi, 53, 20125 Milano ITALY
** See annex of J. Pamela et al, "Overview of JET Results",*
(Proc. 20th IAEA Fusion Energy Conference, Vilamoura, Portugal (2004).

Preprint of Paper to be submitted for publication in Proceedings of the
SOFT Conference,
(Warsaw, Poland 11th – 15th September 2006)

ABSTRACT.
In the framework of the Enhancement Projects at JET, an extension of the capabilities of the Martin-Puplett interferometer has been required for the spectral analysis of the ECE perpendicular and oblique signals. That has been only possible with a complete redesign of the collection optics system. The new instrument is designed to analyze the incoming radiation from standard perpendicular view (two channels) and from oblique view of the ECE radiation at two different angles (four channels) at ~10° and ~22° from the major radius in the toroidal plane. The new optical scheme needed a totally new mechanical layout of the system. This work deals with the detailed description of the mechanical realization and the first characterization of the system.

1. INTRODUCTION

In the framework of the New Microwave Access (MWA) in JET [1,2], the pre-existing single channel Murtin-Puplett Interferometer (MPI) for ECE measurements [3] has needed a multichannel extension for oblique ECE. The oblique ECE signals are collected by the new MWA ECE antenna [4] from two different lines of sight, respectively at 10.05^o and 22.26^o from the major radius in the toroidal plane.

The new instrument [5] is designed to analyze the incoming radiation from six channels, two devoted to standard perpendicular ECE and four to oblique ECE. This has been possible only with a complete redesign of the optical system [6] and, as a consequence, a totally new mechanical layout. This paper deals with the mechanical realization, installation and the first characterization of the new hardware.

2. REQUIREMENTS

Since the oblique ECE radiation is elliptically polarized, with a significant variation of the extraordinary (X) and ordinary (O) fractions over the frequency range, at least two linearly polarized orthogonal components have to be analysed. The two linear polarizations are labelled “mostly-O” and “mostly-X” depending on their prevailing mode content at low frequency. Moreover, at least one standard radial line of sight (X-mode emission) must be preserved for comparison with the oblique signals. An arrangement for a second radial line has foreseen in the system.

All six MPI channels share the existing rotating rooftop mirror (as the moving arm of the interferometer) composed of four 30mm wide helicoidal sectors, with a slope of 4.85^o, arranged on a wheel of 300mm diameter.

The frequency band of interest is 75-400GHz.

3. DESIGN CHOICES

The two input waveguides for oblique ECE are smooth circular with 27.75mm i.d., parallel to the axis of the wheel. For radial ECE, the input waveguide is a standard rectangular S-band WR284, used in TE01 mode, perpendicular to the wheel’s axis.

The output radiation is fed to the He cooled InSb detectors with copper waveguides 12mm i.d. (standard diameter copper pipe closest to the detectors' size).

A confocal system, made of elliptical mirrors, was designed to make performance nearly frequency-independent. The optical scheme is based on two confocal periscopes to achieve an optimum coupling with the input/output waveguide. The focal length of 200mm was chosen for compactness, while allowing to accommodate nearly 50 optical components. The focal length for the final mirror before the output waveguide is 86.486mm. These lengths dictate the distances between the optical points along the rays.

The best coupling between a TE11 and the first Gaussian mode is 86.6% for a ratio of waist to waveguide radius w/a=0.768. The beam truncation at the input waveguide is therefore 2a/w=2.6, and this ratio was used throughout the system to dimension the optical surfaces.

Both lines of the oblique ECE radiation are separated into two linear components with a polarizer grid placed after the first elliptical mirror. The angle between the transmitted and reflected beams was chosen arbitrarily at 90°. In order to get a full back-reflection on the wheel rooftop, the input raypath projection on the wheel plane must be along the tangent to the rooftop vertex. The arrangement of each pair of oblique channels coming from the same waveguide is rigidly fixed by these constraints. The two pairs are placed in radially opposite directions on the wheel, preserving axial symmetry with respect to its axis. The space between them was used for fitting the perpendicular ECE channels (Fig.1).

The waveguide routing of oblique ECE channels was designed to have the axes of the polarization ellipse at +/−45 deg from vertical at the input ports of the instrument, as required for its operation. But the geometry fixed above makes impossible a perfect polarization balance between reference and moving arm of each interferometer. For ideal balance, the input polarization of a rooftop reflector requires should be at 45 deg from the corner. In this case a difference of up to 12 deg is present. As a consequence, all channels have a slight power imbalance that can reduce the fringe amplitude by up to 8% with respect to the ideal case.

4. MECHANICAL LAYOUT

Most optical points can be ideally grouped in three planes, one parallel to the axis of the wheel and two perpendicular, close to each other. A rigid layout was chosen to achieve an alignment-free system in order to avoid re-alignment of a large number of components and to endure the accidental vibrations without loss of performance.

This layout solution makes possible the removal of the whole instrument to gain access to the rotating reflector without losing the correct alignment from the rotating mirror structure.

Each optical component (mirrors, beam splitters) must be positioned precisely to satisfy the critical constraints. For this reason a set of supports was used wedges to give the proper orientation and height to some mirrors. The non-modularities were concentrated in a small number of pieces and the number of different pieces was minimized.

The electromagnetic simulations set the limits for the acceptable mechanical tolerances. The tolerance required in linear dimensions is d_x<0.1mm for any stand-alone component. Parallel and non-parallel faces of each component are required to be manufactured with a tolerance of $d\theta < 0.05$ deg. The required tolerance is obtained using two dowel pins on each component.

A new and more robust enclosure was made for the rotating reflector. It incorporates Mylar windows, encoder support, and acts as a mechanical reference for positioning the system. The motor and wheel were lifted by 100mm to accommodate the new optical system.

The layout of the mainframe is made of two aluminium 5080 optical planes in a "T-shaped" arrangement facing the rotating mirror, one of them holding components on both faces. The planes are positioned on the optical table with two regulated slides and roller mounts. A spacer is mounted on the wheel bearing support and acts as position reference for the new planes. Two "V" shaped struts hold the two planes perpendicular.

The first layer of components, facing the wheel, contains power splitters (rectangular 45° wire grids), the interferometer reference arms (rooftop mirrors with translation stages) and the mirrors of output periscopes. The second layer, mounted on the opposite side of the plane contains input/output waveguide supports, input periscope mirrors, oblique ECE beam splitters and output grids (Fig. 3).

The layer on the other plane holds the input optics for perpendicular ECE channels. It matches the rectangular waveguide with the same optical system used from the oblique channels: the waveguide is tapered into square and the first elliptical mirror is replaced with a parabolic one (focal length of 480mm). A few flat mirrors are inserted to fold the ray trajectory for compactness. Some free space was available on this layer, so a second set of matching optics was accommodated, allowing a second rectangular waveguide to be connected if necessary. Moving a flat mirror and a polarizer grid in a different location, a multiple configuration is possible: it can be used to view O and X mode simultaneously from a single input waveguide, or either mode from two different waveguides.

5. OPTICAL ALIGNMENT

A first check of the system installation is the correct alignment of optical surfaces for each channel. The required test equipment consists of two lasers of two different wavelengths and the optical beamsplitters replacing grids and mechanically identical to them. Each laser is aligned to the system better than 0.5mm/m.

The laser spot must be at the centre of each optical surface. The measured deviation from the optimal position is less than 0.5mm in all the cases, being the maximum tolerable deviation 1mm.
The tests accomplished onto 5 channels displayed a few optical surface misalignments, that were recovered inserting 0.1-0.7mm shims between mirrors and supports. The reason for the misalignments (under assessment) can lie in inaccurate manufacturing of mirror surfaces and/or in insufficient mechanical tolerances. Furthermore, the mirror surface finish, while adequate for microwaves, diffuses light, making the optical alignment difficult. A set of optical high quality mirrors is being considered to make the optical alignment easier since the mirrors used at present diffuse the laser light.

The optical surface of the two mirrors was measured with a laser profilometer. One of them showed a serious defect (Fig.4) introducing an angular error of about 0.34 deg in the direction of the reflected beam.

6. ELECTROMAGNETIC TESTS

The most precise measure of the alignment of the interferometer section is the ratio between the experimental fringe amplitude and the computed maximum given the available power in the interferometer arms. The result should be compared with the computed power imbalance given from the simulations (Table 1). The tests were made using a power modulated 110GHz Gunn.

7. LOSSES

The global alignment of the optical system (excluding the interferometer section) is best assessed by the throughput (insertion loss). The system throughput was measured with a blackbody source (600°C) viewed through a chopper. The peak-to-peak detector response was measured when the source was at the input waveguide and at (a mock-up of) the output waveguide. The ratio of amplitudes is an estimate of the insertion losses. The tests were made for the channels with the shortest/longest output waveguide path. The results show an insertion loss of ~13 dB for every channel (including the long over-sized input waveguide and the output waveguide), about 6 dB of which being due to the output waveguide alone.

The optical system loss was also measured [7], for the oblique channels only. A modulated noise source (110-170 GHz) was placed before and after the optical system. The coupling losses of the four oblique channels are between 1.2 and 2.5dB, in close agreement with simulations. Removing the (estimated) input waveguide loss from the blackbody measurements mentioned above, one can estimate the optical system loss independently. The results, while affected by a large error bar, agree with simulations and the other measurements. (Fig.5)

The influence of loose connections in the output waveguide was estimated too. The measurements were made with the output waveguides properly connected, totally disconnected and with one loose connection. A single loose connection can account for ~1 dB losses.

CONCLUSIONS

The system has been correctly assembled and installed at JET. Characterization measurements show that the performance of four channels out of five is better than 90% of the design value and one mildly satisfactory.

The position of a few optical surfaces was found to be misaligned and the reason is under investigation. Inaccurate mirror manufacturing is suspected. A set of optical high quality mirrors is being considered to make the optical alignment easier.

The measures of optical system loss agree with simulation within error bars.

ACKNOWLEDGMENTS

The authors are indebted to Mr J. Fessey for his support and valuable suggestions, Mr P. Trimble for his assistance during the installation and Dr G. Grossetti for the insertion loss measurements.

REFERENCES

[1]. L.Cupido et al, Fusion Engineering and Design, **74** 707-713 (2005)

[2]. E. de la Luna et al, Recent developments of ECE diagnostics at JET, EC-13, 2004

[3]. M. Zerbini et al, 15th Topical conf. on High Temperature Plasma Diagnostics, 2004

[4]. C. Sozzi, A. Bruschi, A. Simonetto et al, Fusion Eng. Des. **74**, 691-696 (2005)

[5]. C. Sozzi, A. Simonetto, S. Garavaglia et al, The Multichannel Extension Of The Martin-Puplett Interferometer For Perpendicular And Oblique ECE Measurements On JET, EC-14, 2006

[6]. A. Simonetto, C. Sozzi, S. Garavaglia et al, Conceptual Design Of The Optical Scheme For A Multichannel Martin Puplett Interferometer For Perpendicular And Oblique ECE Measurements On JET, EC-14, 2006

[7]. G. Grossetti, Insertion loss measurements on KK5 interferometer, private communication, 2006

ECE Channel	Reference/ Movable arm Power fraction (measured) (%)	Reference/ Movable arm Power fraction (design) (%)	Fringe Ampltidude design/ideal (%)	Fringe Ampltidude measured ideal (%)	Fringe Ampltidude measured ideal (%)
~20° Mostly X	41,5/58,5	37,9/62,1	95,8	92,2	96,2
~20° Mostly O	31,6/68,4	30,89/69,1	94,1	92,2	98,0
Perpendicular X	21,9/78,1	39,75/60,25	85,4	73,4	85,9
~10° Mostly X	63/37	62,1/37,9	95,8	91,8	95,8
~10° Mostly O	52,8/47,2	60,25/39,75	94,1	86,2	91,6

Table 1: Columns 2-3 measured and computed power fractions in the two arms of interferometers; column 4 is the fractional fringe amplitude as given by the design, column 5 is ratio between the measured fringe amplitude and the maximum available with the given power imbalance and column 6 is the actual performance of each channel.

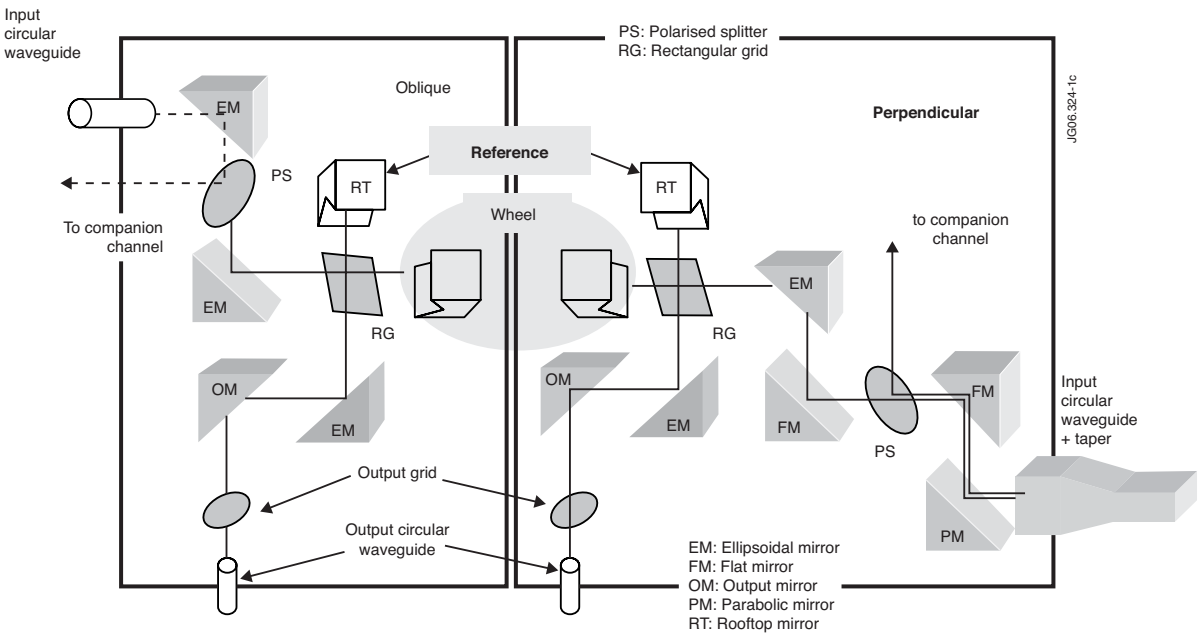

Figure 1: View of the optical scheme.

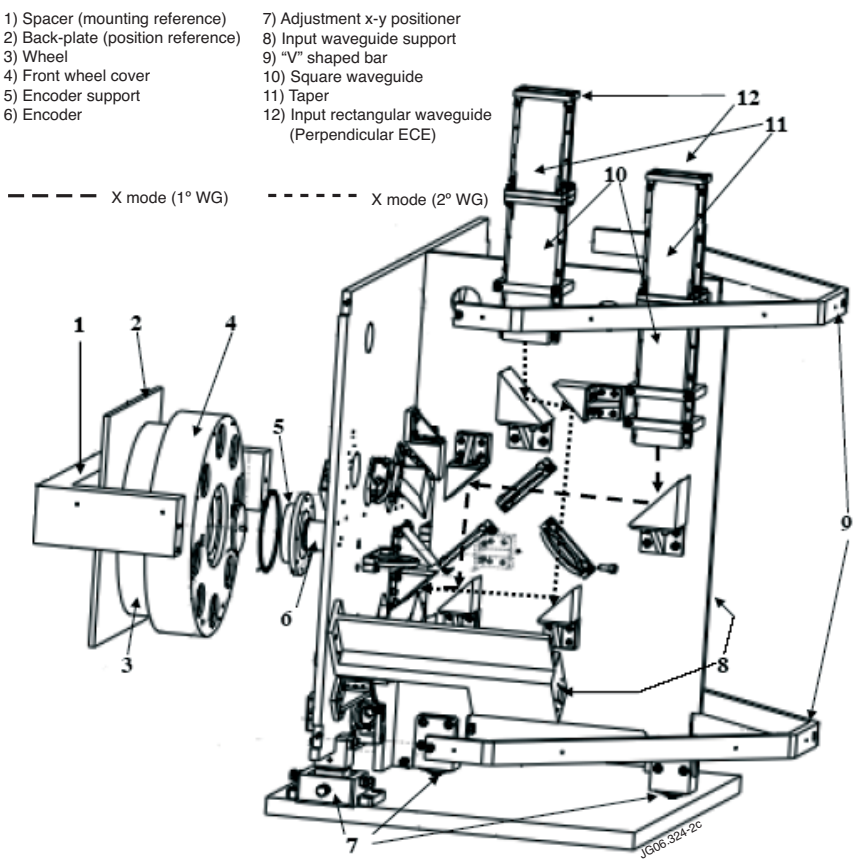

Figure 2: Exploded view of the interferometer.

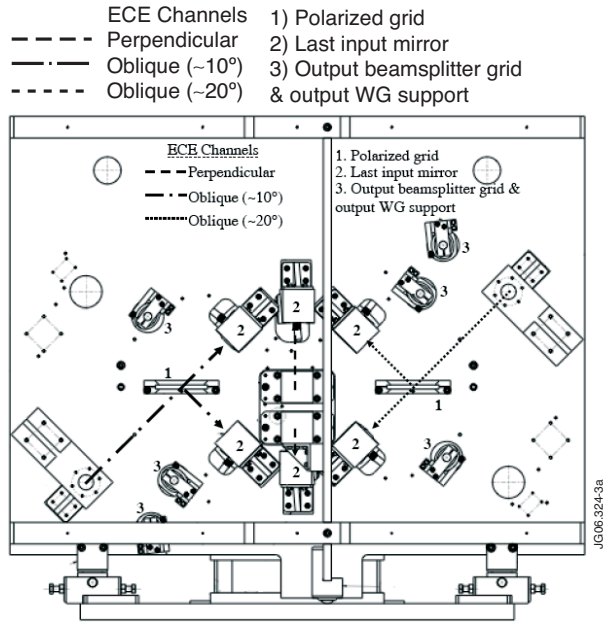

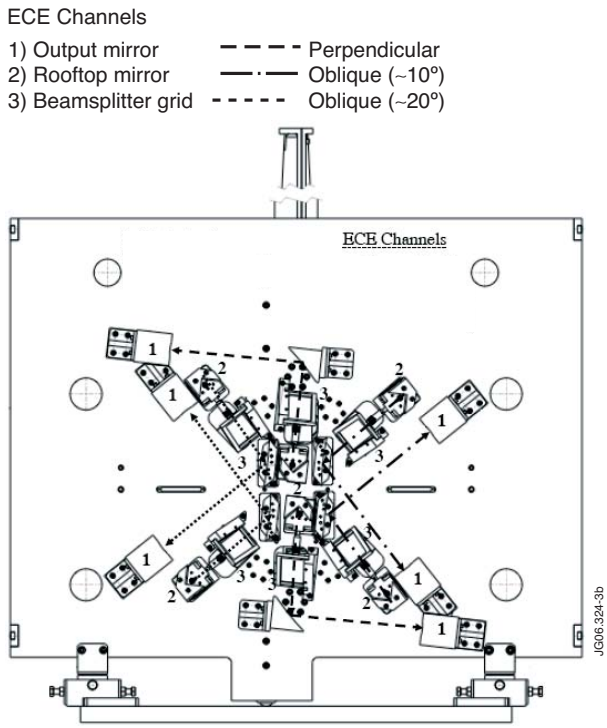

Figure 3: Main frame layout: front view and rear (facing the wheel).

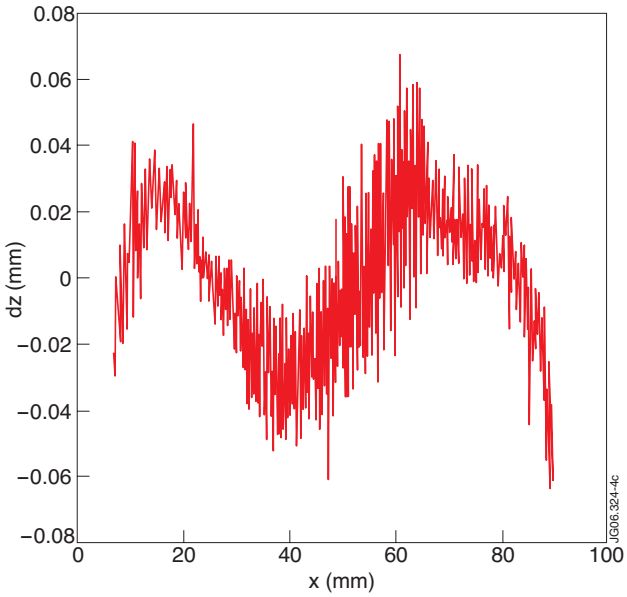

Figure 4: Difference between the real and the computed surfaces along the meridian plane of the ellipsoid. The 0.17deg slope of the central part causes a 0.34deg deviation in the reflected beam.

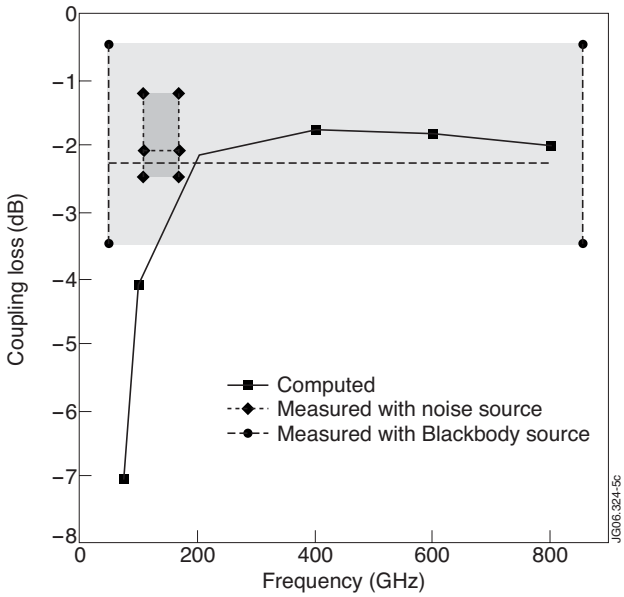

Figure 5: Coupling losses for oblique ECE channels. Shaded areas indicate the error bars in the measures.